Flatness of the setting Sun

Z. Néda[a] and S. Volkán-Kacsó
Department of Physics, Babeş-Bolyai University, RO-3400, Cluj, Romania

(Received 19 April 2002; accepted 1 November 2002)

The flattened rim of the setting or rising Sun is a consequence of atmospheric refraction. We study the flatness as a function of the Sun's inclination angle, the observation height, and the meteorological conditions characterized by pressure, temperature, and lapse rate using a standard model of the atmosphere. Numerical calculations are compared with simple observations. Extreme and unusual situations are revealed.
[DOI: 10.1119/1.1533054]

I. ATMOSPHERIC REFRACTION AND THE SETTING SUN

The refractive index of dry air is very close to unity. Its small variation as a function of temperature and pressure leads to a refractive index gradient in the atmosphere. Although this gradient is very small, atmospheric refraction (bending or dispersion) can be observed due to the large distances traveled by the light in the atmosphere.[1] Atmospheric refraction is responsible for the scintillation of stars, mirages, the puzzling and spectacular green flash, the difference between the apparent and real position of stars, and the flattened rim of the Sun near the horizon.

In this paper we study this last phenomenon and calculate the flatness as a function of the position of the Sun, the altitude of the observer, and meteorological conditions. A similar study, considering fixed atmospheric conditions, was recently published.[2] Here we make a more complete analysis with a different theoretical approach and simple experiments. Our study is restricted to standard atmospheric conditions with a smooth temperature and pressure profile. Nonstandard, but common, atmospheric profiles lead to nonstandard distortions of the solar rim,[3] and are not addressed here.

The paper is structured as follows. We introduce the model of the atmosphere in Sec. II, and the refractive index profile is given. In Sec. III we present a method for calculating the ray path in this model atmosphere and in Sec. IV the flatness of the solar rim is computed. Results for different meteorological conditions and observation altitudes are presented in Sec. V. We describe in Sec. VI our photo and video experiments and compare the measured flatness with theoretical predictions. Finally, we discuss extreme and unusual conditions that are illustrated by pictures, videos, and computer simulations on our Web site.[4] Parts of these documents are also available on EPAPS.[4]

II. THE OPTICAL ATMOSPHERE MODEL

The refractive index n of dry air depends slightly on pressure and temperature and follows Edlen's semi-empirical law:[5]

$$n=1+\left(C_1+\frac{C_2}{\lambda^2}\right)\frac{P}{T}, \tag{1}$$

where $C_1=7.762\times10^{-7}\ \mathrm{K\,m^2/N}$, $C_2=4.36\times10^{-21}\ \mathrm{K\,m^4/N}$, λ is the wavelength of the light, P is the pressure, and T is the absolute temperature. Because the pressure and temperature vary within the atmosphere, we obtain a refractive index gradient which is responsible for atmospheric refraction.

The atmosphere of the Earth extends up to a few hundred kilometers from the surface. As a function of altitude, several layers with different physical properties are distinguishable, as summarized in Fig. 1. From the viewpoint of atmospheric refraction only the first two layers, the troposphere and the stratosphere, are important. In the upper layers of the atmosphere the air is so rarefied that the refractive index can be considered to be unity within a good approximation.

An accepted and widely used model for the atmosphere is the U.S. Standard Atmosphere, established in 1953 and revised in 1976.[6] This model consists of single profiles, representing the idealized steady-state atmosphere for moderate solar activity. Its parameters include the temperature, pressure, density, gravitational acceleration, mean particle speed, mean collision frequency, and mean free path as a function of altitude. In our study we consider an atmosphere model with spherical symmetry, so that all relevant physical quantities (temperature and pressure) vary only as a function of altitude.

We calculate the refractive index of air as a function of altitude as follows. As suggested by the U.S. Standard Atmosphere model, the temperature in the troposphere linearly decreases with a rate of $\kappa=6.5$ K/km and is constant within the tropopause. Although the temperature increases as a function of altitude in the stratosphere, we will follow the work of Thomas and Joseph[2] and assume that the temperature is constant in this region, too. This assumption is fully justified, because the air is so rarefied in this region that the refractive index is already very close to 1. Taking the temperature as constant will not alter the refractive index profile in a noticeable manner. Above the stratosphere ($z>z_s\approx50$ km), we assume that $n=1$, and do not calculate it from Eq. (1). In the context of atmospheric physics the rate of change of a meteorological element with height is called the lapse rate. In our method we assume that the lapse rate of the temperature in the troposphere is $\kappa=6.5$ K/km and it is zero in the tropopause and stratosphere. Up to the top of the stratosphere the temperature profile is therefore given as

$$T(z)=T(0)-\kappa z \quad (z<z_t), \tag{2a}$$

$$T(z)=T(0)-\kappa z_t \quad (z_t\leqslant z\leqslant z_s), \tag{2b}$$

where z is the altitude relative to sea level, and $T(0)$ is the temperature measured at sea level.

For the pressure profile we use a modified barometric formula that takes into account the variation of temperature with altitude as well. Let us consider a slice of air of vertical thickness dz. The variation of pressure within this slice is due to the hydrostatic pressure and is given by

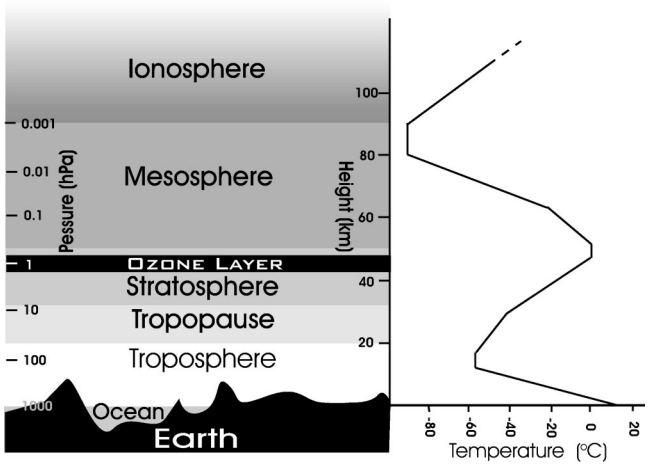

Fig. 1. Distinct layers of the atmosphere and the standard temperature and pressure profile.

$$dP(z) = -\rho(z)g(z)dz, \tag{3}$$

where $g(z)$ is the gravitational acceleration and $\rho(z)$ is the density of air at height z:

$$\rho(z) = \frac{M}{V} = \frac{Nm}{V} = \frac{P(z)m}{kT(z)}. \tag{4}$$

We denote by m the mass of one molecule, N the number of molecules in volume V, $T(z)$ the temperature at height z, and k Boltzmann's constant. Because we focus on the troposphere and stratosphere only, z is small compared to the radius of the Earth ($R \approx 6378$ km). Therefore, the gravitational field g can be considered constant. Thus, we can write

$$dP(z) = -\frac{P(z)mgdz}{kT(z)}. \tag{5}$$

If we use the temperature profile given in Eq. (2) and integrate Eq. (5) between a height zero (sea level) where the pressure is $P(0)$ and an arbitrary height z, we obtain the barometric formula:

$$P(z) = P(0)\left[1 - \frac{\kappa z}{T(0)}\right]^{mg/k\kappa} \qquad (z < z_t), \tag{6a}$$

$$P(z) = P(0)\left[1 - \frac{\kappa z_t}{T(0)}\right]^{mg/k\kappa} \times \exp\left(-\frac{mg(z-z_t)}{k(T(0)-\kappa z_t)}\right) \qquad (z_t \leqslant z \leqslant z_s). \tag{6b}$$

If we substitute this result together with Eq. (2) into Eq. (1), we obtain the refractive index n as a function of the height z. The refractive index profile calculated in this manner for the parameters of the U.S. Standard Atmosphere is given in Fig. 2.

III. TRAJECTORY OF A LIGHT RAY IN THE ATMOSPHERE

We now study the path of a light ray in the optical atmosphere model introduced in Sec. II. Our approach is based on Fermat's principle.[7] An alternative and better known method can be found in Ref. 8. To avoid discussing dispersion, we will consider monochromatic light rays.

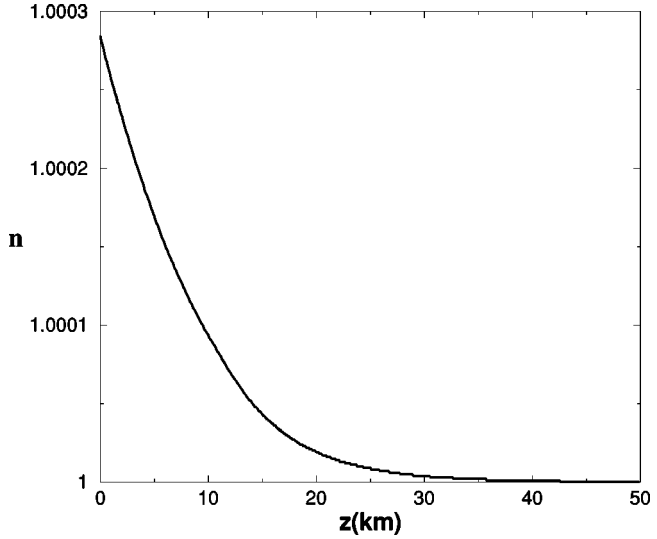

Fig. 2. Refractive index profile for $T(0) = 10\,^{\circ}\mathrm{C}$, $P(0) = 1$ atm, $\kappa = 6.5$ K/km, and $\lambda = 500$ nm.

Let us use the geometry in Fig. 3. An observer at M (altitude z_0) detects the light source placed at S_r (height z'). In the following we will use the notation $P(0)$ and $T(0)$ for the pressure and temperature at sea level, and denote by z_0 the height of the point where the observation is made (which is not always sea level).

Let the arc S_rM be the presumed path of a light ray between S_r and M. The observer detects this light ray in the MS direction, which is tangent to the ray path in M. The source will be seen at S by the observer. (SO and S_rO have radial directions, and thus the light rays in these directions would not bend in our optical atmosphere model.) We denote by δ the apparent inclination angle, characterizing the direction of the S image. Let δ_{dev} be the deviation angle of S relative to the real MS_r direction of the source. The MS_r direction is characterized by δ_r. Following Ref. 2, we compute δ_{dev} as a function of δ.

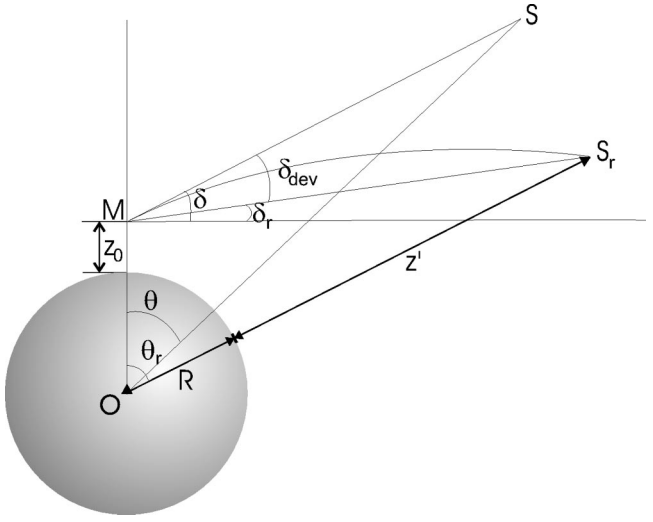

Fig. 3. Real (S_r) and apparent (S) position of a distant source, as observed from the point M within the Earth's inner atmosphere.

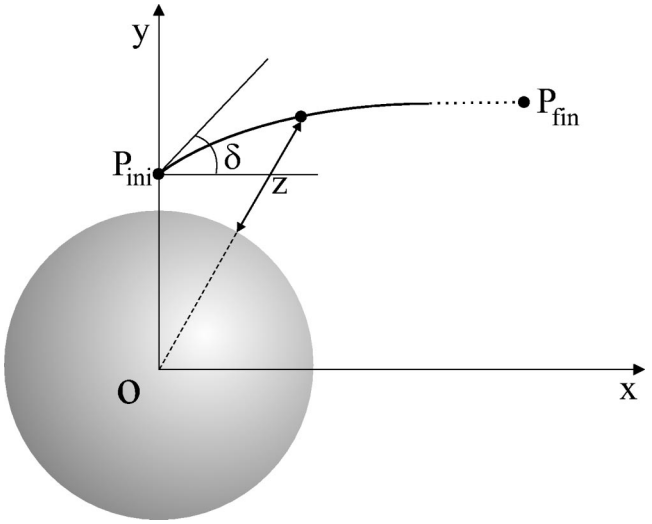

Fig. 4. Geometry and notation for our method based on Fermat's principle.

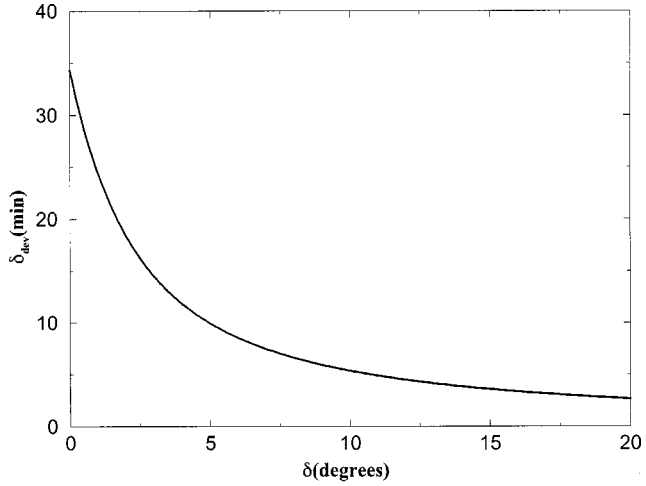

Fig. 5. Deviation angle δ_{dev} between the apparent and real location of a point-like source far from Earth as a function of the apparent inclination angle δ. [$T(0)=10\,^{\circ}\text{C}$, $P(0)=1$ atm, $\kappa=6.5$ K/km, and observation from sea level.]

If the trajectory of a light ray traveling in the X-O-Y plane is described by $y=y(x)$ (see the geometry in Fig. 4), by the use of the Fermat's principle[7] (see the Appendix), we obtain a second-order differential equation for $y(x)$:

$$y''(x)=\frac{\partial n}{\partial z}[x,y(x)]\frac{[1+y'(x)^2]}{n(x,y(x))\sqrt{x^2+y(x)^2}}[y(x)-xy'(x)]. \tag{7}$$

In Eq. (7) $n(x,y(x))$ denotes the refractive index of the air at $x,y(x)$. In our case n can be considered to have spherical symmetry, depending only on the altitude $z=\sqrt{x^2+y(x)^2}-R$.

If we take the $n(z)$ refractive index profile from the atmosphere model of Sec. II, Eq. (7) can be integrated numerically. We start from $P_{\text{ini}}\equiv M(x_0,y_0)$ and assume the initial derivative $\tan\delta=y'(x_0)$. We now construct the $y(x)$ trajectory numerically up to an altitude $z\geqslant z_s$, where we assumed $n(z)=1$. The derivative of $y(x)$ at this point will determine the angle δ_r. For $z>z_s$, the trajectory of the light ray is linear. If we assume that S_r is very far from the Earth ($z'\gg R$), we find that δ_r equals the value used in Fig. 3. The deviation angle $\delta_{\text{dev}}=\delta-\delta_r$, and the desired $\delta_{\text{dev}}(\delta)$ dependence is determined numerically.

For the parameters of the U.S. Standard Atmosphere [$T(0)=10\,^{\circ}\text{C}$, $P(0)=1$ atm, $\lambda=500$ nm and $\kappa=6.5$ K/km] and observations at sea level ($z_0=0$) results for $\delta_{\text{dev}}(\delta)$ are plotted in Fig. 5. These results are in excellent agreement with those given by Thomas and Joseph[2] and the report of the U.S. Naval Observatory.[9] From Fig. 5 we see that the deviation angle is usually quite small, and becomes important only when viewing objects in the vicinity of the optical horizon. The deviation angle increases rapidly for small inclination angles. This effect is responsible for the flattened shape of the rising (or setting) Sun and Moon, and also for the fact that these objects appear more flattened at their bottom. It is interesting to note here that the angular extent of the Sun and full-Moon is $0.53^{\circ}=32'$, and the maximum deviation angle obtained for standard conditions is $0.57^{\circ}=34.5'$. This observation leads us to the interesting result that the entire rim of the Sun or Moon is visible even when in reality it is below the geometrical horizon.

IV. COMPUTING THE FLATNESS

Once we have determined the deviation angle δ_{dev} as a function of the apparent inclination angle δ, it is easy to study the apparently flat rim of the setting Sun. Atmospheric refraction influences only the vertical angular extent d_v of the Sun (Moon), which becomes smaller than the horizontal extent d_h. The flatness of the rim can be characterized by the ratio

$$\alpha=\frac{d_h}{d_v}. \tag{8}$$

Because both the Sun and full Moon are normally visible for the angular extent $d_n=0.53^{\circ}$, we have $d_h=d_n$. The value of d_v can be derived after determining the apparent inclination angle δ as a function of the real inclination angle δ_r, that is, $\delta=F(\delta_r)$. If the apparent inclination angle for the bottom of the Sun is δ_b, corresponding to a real inclination angle δ_{rb}, then $d_v(\delta_b)=F(\delta_{rb}+d_n)-\delta_b$, and

$$\alpha(\delta_b)=\frac{d_n}{F(\delta_{rb}+d_n)-\delta_b}. \tag{9}$$

For fixed observation altitude and meteorological conditions, the maximal possible flatness α_c corresponds to the situation when the bottom of the Sun touches the horizon. This happens for a critical inclination angle $\delta_b=\delta_c$.

By decreasing δ in small steps (in our calculations 0.01°), and applying our method for computing the light ray trajectory, both the function $\delta=F(\delta_r)$ and δ_c can be determined numerically.

V. THEORETICAL RESULTS

We now study the flatness α_c of the rim as a function of the observational altitude and the pressure and temperature. It is also shown that the value of α is insensitive to details of the optical atmosphere model, indicating the reliability of the

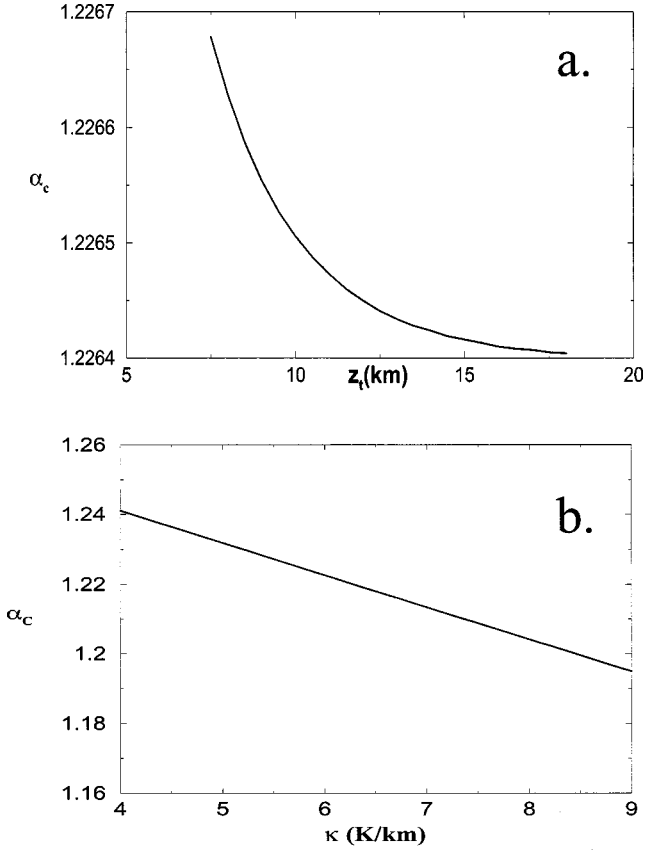

Fig. 6. Maximal observable flatness, α_c, as a function of (a) z_t, the height of the troposphere, and (b) the lapse rate κ. [$T(0)=0$ °C, $P(0)=1$ atm, observation from sea level, normal lapse rate for (a) and $z_t=14$ km for (b).]

results. We considered monochromatic light with wavelength $\lambda=500$ nm, corresponding to the color green, for our calculations.

A. Sensitivity of the optical atmosphere model

To calculate the refractive index profile, we need several results from the U.S. Standard Atmosphere model, namely, the height of the troposphere z_t, the height of the stratosphere z_s, and the lapse rate κ. It is evident that the exact value of z_s does not significantly influence our results, because in the stratosphere the refractive index is already 1 to a good approximation.

We first study the influence of z_t on α_c. We considered normal conditions with $T(0)=0$ °C, $P(0)=1$ atm, observations at sea level, and a standard lapse rate $\kappa=6.5$ K/km. As illustrated in Fig. 6(a), the value of z_t (in a reasonable range) has no significant influence (note the scale on the vertical axis). The value of κ has a more noticeable effect on α_c [see Fig. 6(b)], but this variation is also small for the practically important fluctuations around the standard value ($\kappa=6.5$ K/km). We conclude that our results are insensitive to the details of our optical atmosphere model. If otherwise not specified, we chose the height of the troposphere to be $z_t=14$ km and the height of the stratosphere to be $z_s=50$ km.

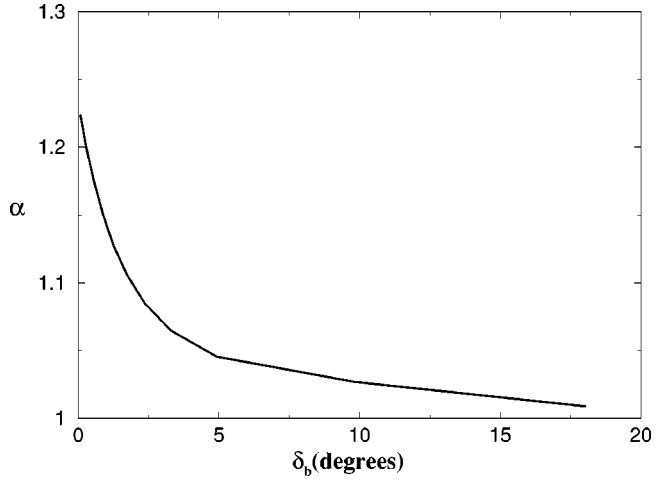

Fig. 7. Observable flatness, α, as a function of the δ_b, the inclination angle of the bottom of the Sun. [$T(0)=0$ °C, $P(0)=1$ atm, observation from sea level and standard lapse rate.]

B. Flatness as a function of the inclination angle and observation height

We next present results for α as function of the apparent inclination angle of the Sun's bottom. Results for $T(0)=0$ °C, $P(0)=1$ atm, $\kappa=6.5$ K/km and observations at sea level are summarized in Fig. 7. As already emphasized, the asymmetric rim of the setting (or rising) Sun becomes evident only for very small values of δ_b, when the Sun is close to the horizon. For these normal atmospheric parameters we find that $\alpha_c\approx 1.2$.

We now assume that the observer is at height z_0 above sea level, and there is no obstacle in the direction of the horizon, which is at sea level. It is obvious that for higher altitudes, the critical angle δ_c will be smaller (and become negative) and the deviation angle increases even more rapidly in the neighborhood of δ_c. This result leads us to the conjecture that the observed flatness should also be larger. We take $T(0)=0$ °C and $P(0)=1$ atm, the normal atmospheric conditions at sea level, and $\kappa=6.5$ K/km, and calculate the maximal observable flatness α_c as a function of observation height. Our results are plotted in Fig. 8. As expected, α_c increases with z_0. We find that from the top of a 5 km high mountain, we would observe $\alpha_c\approx 1.5$, and from a commercial flight at 10 km height at sunset, we would detect a maximal flatness $\alpha_c\approx 1.7$. For altitudes of 40 km, we can obtain extreme values of $\alpha_c\approx 2.5$.

C. Influence of temperature and pressure

The temperature $T(0)$ at sea level influences the results on the observed flatness. For observations at sea level, normal $P(0)=1$ atm pressure, and the standard $\kappa=6.5$ K/km lapse rate, the temperature dependence of α_c is presented in Fig. 9(a). For $T=30$ °C, $\alpha_c\approx 1.1$, but for $T(0)=-40$ °C, it becomes 1.3, and increases rapidly for lower temperatures (arctic conditions).

Increasing the pressure $P(0)$ at sea level results in the increase of the observable flatness, α_c. For a reasonable range of $P(0)$, $T(0)=0$ °C, observation at sea level, and the

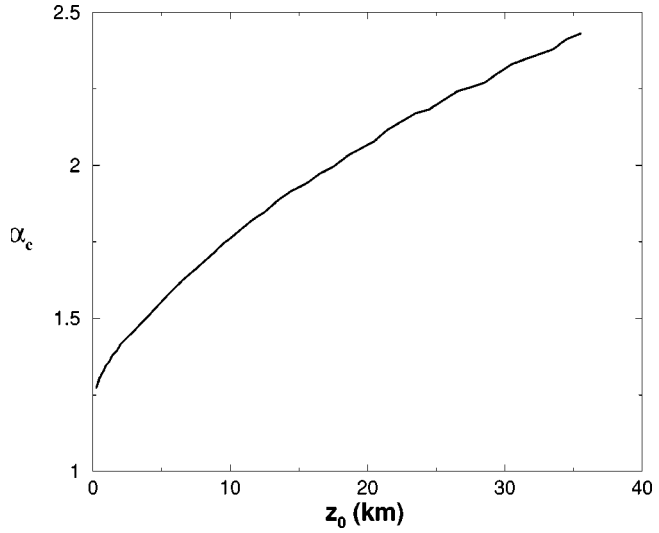

Fig. 8. Maximal observable flatness, α_c as a function of the observation height z_0. [$T(0)=0$ °C, $P(0)=1$ atm and $\kappa=6.5$ K/km.]

standard temperature lapse rate, the variation of the flatness α, as a function of $P(0)$, is given in Fig. 9(b).

D. A simulation

We also have developed software that computes and visualizes the rim of the setting Sun. After choosing the temperature and pressure and observation height, the user can follow how a sunset might look in our optical atmosphere. The Windows program can be downloaded from the Web site accompanying this paper.[4]

VI. THE REALITY

It is relatively easy to measure the flatness of the setting (or rising) Sun. We took photos and videos and analyzed them as a function of the inclination angle of the Sun. To obtain a nicely visible rim, we used a solar filter and studied mainly small inclination angles δ_b, where the light intensity was low. With appropriate solar filters and a calibrated eyepiece, telescope observations were also possible. To keep our eyes safe, the choice of an appropriate solar filter is crucial for the telescope observations. These filters must stop infrared radiation, have a small transmittance (usually smaller than 0.1%), and a small bandwidth (usually smaller than 10 nm) to ensure a detectable rim. The best solution is to use a brand-name filter, specially designed for telescope observations of the Sun. We used an available blue-glass JMB-binocular solar filter with 0.1% transmittance and a 5 nm bandpass.

When the Sun is close to the horizon, the inclination angle of the Sun can be determined from these pictures. The horizontal angular extent of the Sun always corresponds to $d_n=0.53°$. On the pictures the distance of the Sun from the horizon l_s, can be compared with the horizontal extent of the setting Sun l_n, and the inclination angle results from here as $\delta_b=d_n l_s/l_n$. Doing experiments with the setting or rising Moon is more complicated, because we need a full Moon, we must work at night, and we have to analyze pictures where the horizon is not clearly visible.

We have taken a series of pictures in South Bend, Indiana (altitude 100 m) both in winter and late spring, with different

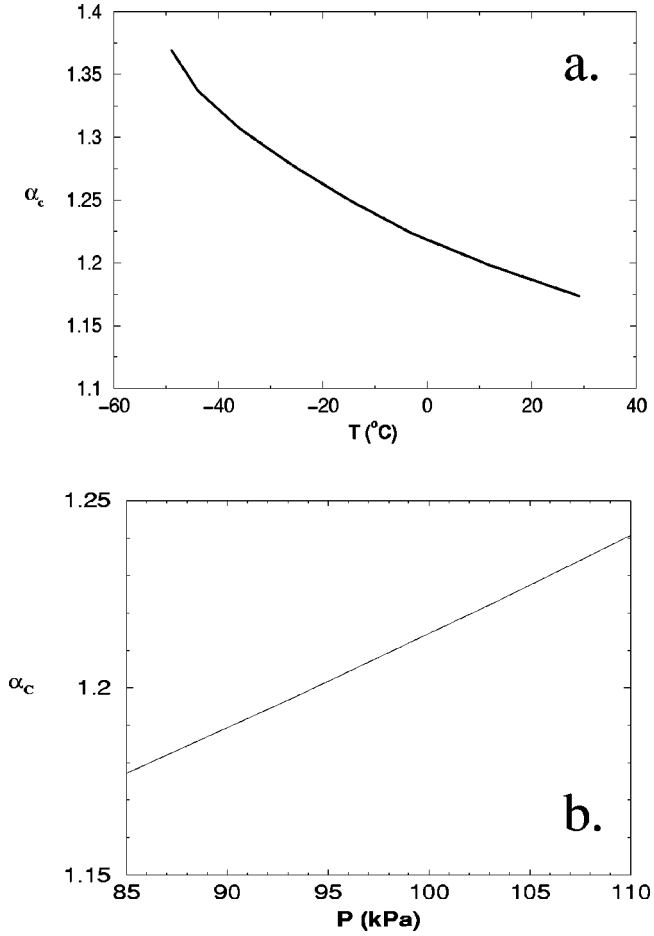

Fig. 9. Maximal observable flatness, α_c, as a function of (a) the air temperature and (b) the pressure at sea level. Observations at $\kappa=6.5$ K/km, $P(0)=1$ atm for (a), and $T(0)=0$ °C for (b).

temperature conditions. As an example of our results, we present in Fig. 10 a series recorded during a sunrise in winter. The mean temperature during the sunrise was -5 °C, and the atmospheric pressure was 103 kPa. During this sunrise the temperature was approximately constant. A similar series from a spring sunset was also analyzed.[4] During this sunset the mean temperature was 12 °C, the atmospheric pressure 98 kPa, and the temperature dropped appreciably during the time the pictures were made.

As an initial confirmation of our theoretical results, we found that for the same inclination angle, the flatness is bigger in winter, that is, for lower $T(0)$ values. Quantitative results for the flatness as a function of the Sun's inclination angle (bottom of the rim) are plotted in Fig. 11 along with

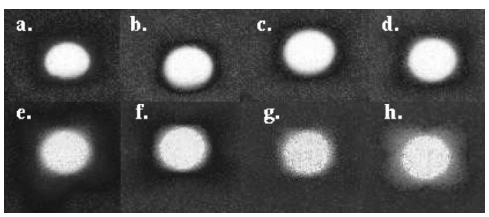

Fig. 10. Rim of the rising Sun for different inclination angle δ_bs: (a) 0.08°, (b) 0.15°, (c) 0.42°, (d) 0.6°, (e) 0.97°, (f) 1.2°, and (g) 1.8°.

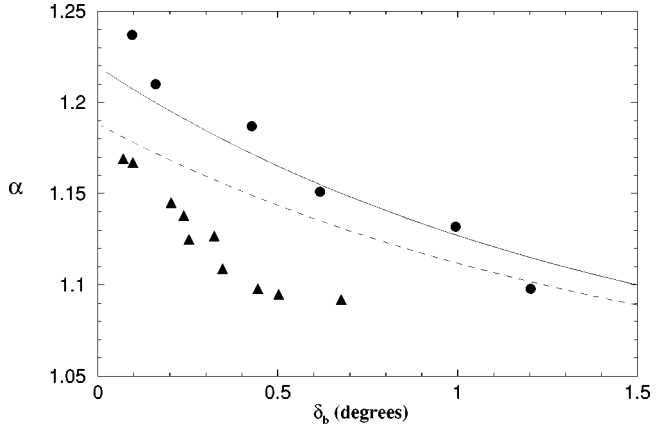

Fig. 11. The flatness as a function of inclination angle. Comparison between experimental results and theory for a sunrise and a sunset photo sequence. The circles are results from sunrise pictures taken in winter with $T(0)=-5$ °C and $P(0)=103$ kPa. The triangles are results from pictures taken in May 2001 with a mean temperature $T(0)=12$ °C and $P(0)=98$ kPa. Observations were made at $z_0=100$ m with the horizon roughly at the same altitude. Theoretical results for the listed atmospheric conditions and $\kappa=6.5$ K/km are plotted by continuous and dashed lines for the winter and spring conditions, respectively.

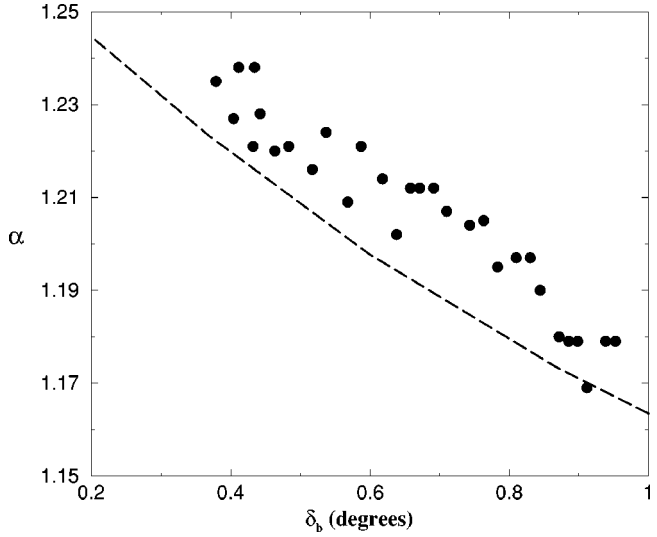

Fig. 12. Results from a video (dots) and theoretical predictions (dashed line) for the flatness as a function of the inclination angle. [$T(0)=7$ °C, $P(0)=100.8$ kPa, observations at $z_0=400$ m, horizon at $z_h=300$ m, and $\kappa=6.5$ K/km.]

our corresponding theoretical results. As seen from Fig. 11 the measured values of α for the winter conditions are in acceptable agreement with the theoretical calculations. However, for the spring series the theoretical values of α are higher and decrease slower as a function of the inclination angle δ_b than the measured data. One reason for this discrepancy is the decreasing temperature during the sunset. If we took account of this decrease in the calculations, it would result in values of α closer to the observations. However, the temperature variation does not explain the constantly lower values measured for α. We conclude that at the time of this measurement, the atmosphere had a refractive index profile different from the one used in our model.

A second set of experiments was done by filming sunsets in Cluj (Romania). The video allowed us to follow more precisely the flatness as a function of the inclination angle. The inclination angle was calculated by the same method as in the photographs, that is, by comparing the height between the bottom of the Sun and horizon with the horizontal extent of the setting Sun. Because Cluj is not a flat region like South Bend, we had to determine the altitude of the optical horizon as well. Our results from the videos in comparison with theoretical expectations (for the appropriate atmospheric conditions) are plotted in Fig. 12. For this measurement good agreement between theoretical and experimental data is achieved. Because the lapse rate for the theoretical calculations was taken from the standard atmosphere model, the obtained small difference is understandable.

Sunset or sunrise (moon-set or moon-rise) is usually a favorite theme for professional and amateur photographers. The Internet is full of beautiful and useful pictures. Many of these pictures are taken under extreme conditions (arctic environment, airplanes, space shuttle, or high mountains), offering an excellent possibility to check our model. Moreover, there are also interesting videos exemplifying how the observed flatness increases in the neighborhood of the horizon. We recommend that the interested reader search the Web for such materials. We have also collected noncopyrighted materials about sunset, sunrise, moon-set, and moon-rise and have classified and stored them on our Web site.[4]

In agreement with our expectations, we found that for a sunrise (or sunset) viewed from a space shuttle, α_c can be greater than 2.5, and in an arctic environment α_c increases up to 1.6. For most of the usual low-altitude photos, we found $\alpha_c \approx 1.1-1.2$. Pictures taken from a commercial airplane yielded $\alpha_c \approx 1.5$. We also found a series of photos for a sunset over the ocean, where the rim of the Sun is clearly visible. The results of our analysis are again in agreement with our theoretical predictions. The videos on our Web site will also convince the reader of the rapid variation of α as a function of δ_b, the inclination angle.

VII. CONCLUSIONS

Atmospheric refraction is responsible for the asymmetric rim of the setting (or rising) Sun. A method for computing the path of a light ray in an optical atmosphere model was presented. By determining the deviation angle between the apparent and real inclination of a point-like light-source, we were able to compute the flatness of the rim. It was found that the maximal flatness obtained in the vicinity of the horizon increases as a function of observation altitude and pressure, and decreases as the temperature increases. We also found that the flatness is rather insensitive to the fine details of the optical atmosphere model, which makes our results robust. Simple observations and pictures from the Internet shows the usefulness of our theoretical predictions. Our analysis also can be effectively used to study atmospheric refraction in nonstandard atmospheric conditions.

VIII. SUGGESTED PROJECTS AND PROBLEMS

By applying the analysis discussed here or by just using the simulation software provided on our Web site,[4] we suggest the following related projects:

(1) Show that the observed flatness also characterizes the apparently slowing angular speed of the setting Sun.

(2) Find extreme conditions under which the observed flatness can become infinite, that is, the Sun looks like a line.
(3) From Eq. (1) it is obvious that atmospheric refraction depends on the wavelength of the light ray, a phenomenon called dispersion. Differently colored light rays coming from a source emitting a continuous spectrum will suffer different deviations. Light with smaller wavelengths (higher frequencies) rays will deviate more strongly, leading to a separation of the colors in the observed Sun. Because the high-frequency visible components (corresponding to violet and blue colors) are strongly scattered by the atmosphere, the green component reaching the observer directly will suffer the most bending. When the Sun disappears below the horizon, this component will be observed leading to a green flash on the horizon.[10] Study the green flash in the standard atmosphere.

ACKNOWLEDGMENTS

This work was supported by the KPI-Sapientia Foundation. We thank the Bergen Computational Physics Laboratory in the framework of the European Community Access to Research Infrastructure of the Improving Human Potential program for access to their supercomputer facilities. We also thank I. Albert and T. Néda for useful discussions and help in the video and photo experiments.

APPENDIX: APPLICATION OF FERMAT'S PRINCIPLE

Fermat's principle[7] states that light travels between two points along the path that requires the least time in comparison to other nearby paths. We can reformulate Fermat's principle by using the optical path instead of time. Let us consider that the trajectory of the light ray in the X-O-Y plane is described by the curve $y=y(x)$ (see Fig. 4). Fermat's principle implies that

$$s=\int_{M(x_0,y_0)}^{S_r(x_f,y_f)} n(x,y(x))\,ds = \int_{x_0}^{x_f} n(x,y(x))\sqrt{1+y'(x)^2}\,dx \tag{A1}$$

should have a local minimum. In Eq. (A1) $n(x,y(x))$ denotes the refractive index of the medium at the point x, $y(x)$. In our case n has spherical symmetry and is a function only of $z=\sqrt{x^2+y(x)^2}-R$.

We can write Eq. (A1) as

$$s=\int_{x_0}^{x_f} f[x,y(x),y'(x)]\,dx, \tag{A2}$$

with

$$f[x,y(x),y'(x)]=n(\sqrt{x^2+y(x)^2}-R)\sqrt{1+y'(x)^2}. \tag{A3}$$

We search for the function $y(x)$ that minimizes s. If we fix two points M and S_r between which the light travels, the minimum of s leads to the classical variational problem

$$\delta s=0, \tag{A4}$$

with

$$\delta[y(x)]|_{x=x_0}=0, \tag{A5a}$$

$$\delta[y(x)]|_{x=x_f}=0. \tag{A5b}$$

The solution of this problem is well known[11] and is given by the second-order differential equation:

$$\frac{\partial f}{\partial y}-\frac{d}{dx}\left[\frac{\partial f}{dy'}\right]=0. \tag{A6}$$

It is straightforward to show that

$$\frac{\partial f}{\partial y}=\frac{\partial n(x,y(x))}{\partial z}\frac{y(x)}{\sqrt{y^2(x)+x^2}}\sqrt{1+y'(x)^2}, \tag{A7a}$$

$$\frac{d}{dx}\frac{\partial f}{\partial y'}=\frac{\partial n(x,y(x))}{\partial z}\frac{y'(x)y(x)+x}{\sqrt{y(x)^2+x^2}}\frac{y'(x)}{\sqrt{1+y'(x)^2}} + n(x,y(x))y''(x)\frac{1}{[1+y'(x)]^{3/2}}. \tag{A7b}$$

By simple algebra we obtain from Eqs. (A6) and (A7) a second-order differential equation for $y(x)$:

$$y''(x)=\frac{\partial n(x,y(x))}{\partial z}\frac{[1+y'(x)^2]}{n(x,y(x))\sqrt{x^2+y(x)^2}}[y(x)-xy'(x)]. \tag{A8}$$

[a]Electronic mail: zneda@phys.ubbcluj.ro

[1]R. Greenler, *Rainbows, Halos and Glories* (Cambridge U. P., Cambridge, 1980). See also A. T. Young, "Annotated bibliography of mirages, green flashes, and atmospheric refraction," ⟨http://mintaka.sdsu.edu/GF/bibliog/bibliog.html⟩.
[2]M. E. Thomas and R. I. Joseph, "Astronomical refraction," Johns Hopkins APL Tech. Dig. **7** (3), 279–284 (1996).
[3]L. Györi, "Determination of atmospheric refraction from the distortion of the Suns disc," Astron. Astrophys. **278** (2), 659–664 (1993).
[4]See EPAPS Document No. E-AJPIAS-71-016302 for a movie sequence for a moonset scenario filmed from the space-shuttle, and some pictures. A direct link to this document may be found in the online article's HTML reference section. The document may also be reached via the EPAPS homepage (http://www.aip.org/pubservs/epaps.html) or from ftp.aip.org in the directory /epaps. See the EPAPS homepage for more information.
[5]B. Edlen, "The refractive index of air," Meteorologia **2**, 71–80 (1966).
[6]*U.S. Standard Atmosphere, 1976* (U.S. Government Printing Office, Washington, DC, 1976).
[7]D. J. Schroeder, *Astronomical Optics*, 2nd ed. (Academic, San Diego, 1999), Chap. III.
[8]W. M. Smart, *Spherical Astronomy*, 6th ed. (Cambridge U. P., Cambridge, 1977).
[9]U.S. Naval Observatory, *The Nautical Almanac* (U.S. Government Printing Office, Washington, DC, 1993).
[10]D. J. K. O'Connel, *The Green Flash and Other Low Sun Phenomena* (North Holland, Amsterdam, 1958). See also A. T. Young, "An introduction to green flashes," ⟨http://mintaka.sdsu.edu/GF/⟩.
[11]G. B. Arfken and H. J. Weber, *Mathematical Methods for Physicists*, 4th ed. (Academic, London, 1995), Chap. 17.